

# Topology optimization of continuum structures subjected to the variance constraint of reaction forces

Tong Gao<sup>1,2</sup>  · Libin Qiu<sup>1</sup> · Weihong Zhang<sup>1</sup>

Received: 20 November 2016 / Revised: 4 April 2017 / Accepted: 13 June 2017 / Published online: 8 July 2017  
© Springer-Verlag GmbH Germany 2017

**Abstract** In this paper, the attainment of uniform reaction forces at the specific fixed boundary is investigated for topology optimization of continuum structures. The variance of the reaction forces at the boundary between the elastic solid and its foundation is firstly introduced as the evaluation criterion of the uniformity of the reaction forces. Then, the standard formulation of optimal topology design is improved by introducing the variance constraint of the reaction forces. Sensitivity analysis of the latter is carried out based on the adjoint method. Numerical examples are dealt with to reveal the effect of the variance constraint in comparison with solutions of standard topology optimization.

**Keywords** Topology optimization · Reaction force · Variance constraint · Sensitivity analysis

## 1 Introduction

In last decades, topology optimization of continuum structures is recognized as a challenging research topic in engineering design community. The standard formulation of compliance minimization with applied mechanical loads was initially developed and then extended to various complicated design problems for the achievement of optimal material layout (Deaton and Grandhi

2014; Sigmund and Maute 2013; Zhu et al. 2015). To this end, much effort was made to develop different formulations with required definitions of objective functions and design constraints.

In static problems, the compliance or strain energy of the whole structure is the most popular objective function and usually minimized to obtain the stiffest structures subjected to the volume constraint (Bendsøe 1989). Recently, the summation of the strain energies of all finite elements within the specific shape preserving zones were assigned as an additional design constraint to control the local deformation (Zhu et al. 2016). Displacement of the given DOF (degree of freedom) was also used (Kočvara 1997). In the case of a single concentrated force, the minimization of the displacement magnitude at the applied node along the direction of the applied force is equivalent to the minimization of the global structural compliance. Stress constraint is another important design criterion and deeply investigated (Cheng and Guo 1997; Duysinx and Bendsøe 1998). Besides, structural topology and support locations were simultaneously optimized (Buhl 2002).

In thermo-elastic problems, the structural compliance (Rodrigues and Fernandes 1995) was also minimized for the stiffest structure. However, it was found that the elastic strain energy minimization and mean compliance minimization led to different configurations (Zhang et al. 2014). Both optimization formulations are equivalent only under pure mechanical loads. Moreover, the minimization of the maximum von-Mises stress was achieved by seeking the uniform energy density (Pedersen and Pedersen 2012). Besides, the magnitudes of the reaction forces at specific nodes were introduced as design constraints to indirectly limit the thermal loading (Deaton and Grandhi 2013).

In dynamic problems, most researches were focused on maximization of fundamental, high-order eigenfrequencies or the gap between two consecutive eigenfrequencies (Díaz and Kikuchi 1992; Hilding 2000). In case of the harmonic or stationary random force excitation, the objective function was

✉ Tong Gao  
gaotong@nwpu.edu.cn

✉ Weihong Zhang  
zhangwh@nwpu.edu.cn

<sup>1</sup> State IJR Center of Aerospace Design and Additive Manufacturing, Northwestern Polytechnical University, Xi'an 710072, China

<sup>2</sup> Institute of Intelligence Material and Structure, Unmanned System Technologies, Northwestern Polytechnical University, Xi'an 710072, China

defined by the so-called dynamic compliance (Jog 2002; Ma et al. 1995) or the displacement amplitude (Liu et al. 2015b; Zhang et al. 2015b).

In stability problems, the buckling critical load constraint was introduced into the topology optimization model (Neves et al. 1995).

Some other design criteria have been studied as well. For multicomponent optimization problems, physical properties, e.g., gravity centre (Zhu et al. 2009) and moment of inertia of a structure (Takezawa et al. 2006) were considered and well recognized in aircraft and aerospace structure designs. In the case of multiple materials, it has been demonstrated that the mass constraint is more beneficial and physically more significant than the volume constraint (Gao and Zhang 2011), although both kinds of constraints are identical when only one single solid material phase is present.

The variance constraint of nodal forces at the interface between the main section and connection section was introduced into the topology optimization formulation as the evaluation criterion in the design of the connection section to transfer concentrated external forces to its main section (Zhang et al. 2015a). In that work, the nodal forces are located at the interface between two elastic solids.

This paper focuses on the design constraint on the reaction forces at the specific fixed boundary, i.e., the reaction forces between an elastic solid and its foundation. According to engineering experience, uniform reaction forces, i.e., uniform stress distribution in the connectors or welds, usually benefit the structural performance (Chang et al. 1999). Particularly, in the long-term usage of high- or ultra-precision machines, an uniform distribution of vertical reaction forces over the pedestal supports greatly avoid non-uniform creep relaxation of the supports that deteriorates the levelness of the bench surface and the machining accuracy (Liu et al. 2015a). The configuration and flexibility of the machine frame remarkably affect the distribution of the vertical loads at each support, which is usually uneven in practice but is treated as uniform forces (Kono et al. 2015). However, the design of the machine frame to improve the reaction forces distribution has not been a popular aspect of optimization design in spite of its significant effect on the long-term performance of machine tools. Therefore, it is of great importance to investigate the appropriate evaluation criterion of the uniformity of the reaction forces and the topology optimization formulation for the machine frame at the early concept stage. This is the motivation of the current work.

This paper is organized as follows. In Section 2, a basic formulation of finite element analysis is firstly presented for calculation of reaction forces. In Section 3, the variance of the reaction forces is introduced as the evaluation criterion of the uniformity of the reaction forces. In Section 4, topology optimization problem subjected to the variance constraint of the reaction forces is formulated. Sensitivity analysis is carried out and detailed in the Appendix. The validity of the proposed

formulation is illustrated with 2D and 3D numerical examples in Section 5. Finally, conclusions are drawn out.

## 2 Finite element analysis

Fig. 1 illustrates a structural domain  $\Omega$  with applied force  $F^a$  and homogeneous Dirichlet boundary condition. The static linear analysis corresponds to the solution of finite element eq.

$$\mathbf{F} = \mathbf{K}\mathbf{U} \quad (1)$$

Herein,  $\mathbf{K}$  denotes the global stiffness matrix.  $\mathbf{U}$  and  $\mathbf{F}$  are the nodal displacement vector and nodal force vector, respectively.

By rewriting the finite element equilibrium equation with the separation of the matrix and vectors, we have

$$\begin{Bmatrix} \mathbf{F}^a \\ \mathbf{R} \end{Bmatrix} = \begin{bmatrix} \mathbf{K}_{cc} & \mathbf{K}_{cs} \\ \mathbf{K}_{cs}^T & \mathbf{K}_{ss} \end{bmatrix} \begin{Bmatrix} \mathbf{U}_c \\ \mathbf{U}_s \end{Bmatrix} \quad (2)$$

with

$$\mathbf{K} = \begin{bmatrix} \mathbf{K}_{cc} & \mathbf{K}_{cs} \\ \mathbf{K}_{cs}^T & \mathbf{K}_{ss} \end{bmatrix} \quad (3)$$

Herein, subscript s and c represent DOFs with and without imposed values, respectively.  $\mathbf{F}^a$  represents the applied load vector and  $\mathbf{R}$  is the nodal reaction force vector.

In this work, homogeneous Dirichlet boundary condition refers to

$$\mathbf{U}_s = \mathbf{0} \quad (4)$$

and (2) can be simplified as

$$\begin{Bmatrix} \mathbf{F}^a \\ \mathbf{R} \end{Bmatrix} = \begin{bmatrix} \mathbf{K}_{cc} & \mathbf{K}_{cs} \\ \mathbf{K}_{cs}^T & \mathbf{K}_{ss} \end{bmatrix} \begin{Bmatrix} \mathbf{U}_c \\ \mathbf{0} \end{Bmatrix} \quad (5)$$

where the following two parts can be used to solve  $\mathbf{U}_c$  and to calculate  $\mathbf{R}$ , respectively.

$$\begin{aligned} \mathbf{F}^a &= \mathbf{K}_{cc} \mathbf{U}_c \\ \mathbf{R} &= \mathbf{K}_{cs}^T \mathbf{U}_c \end{aligned} \quad (6)$$

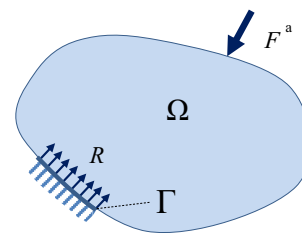


Fig. 1 Illustration of a structure with applied force and homogeneous Dirichlet boundary condition

### 3 Variance of the considered reaction forces

The purpose of this work is to seek the stiffest topology configuration under the applied forces and the constraint of distribution uniformity of the reaction forces. A proper quantitative description of the uniformity of the reaction forces is necessary.

Theoretically, variance is defined as the expectation of the squared deviation of a measurable variable from its mean. It is often used to measure how far a set of variable values are spread out from their mean. Here, the variance of the reaction forces on the specific DOFs is introduced as a measure of the uniformity of the reaction forces.

Assume that  $\Gamma_{RV}$  is the set of the specific DOFs on which the reaction forces are expected to be uniformly distributed. Usually, all reaction forces normal to the fixed boundary are included in  $\Gamma_{RV}$ . And then, the variance of the reaction forces is calculated as

$$D(\mathbf{R}) = \frac{1}{n_r} \sum_j (R_j - \bar{R})^2 \text{ or } D(\mathbf{R}) = \frac{1}{n_r} (\mathbf{R} - \bar{\mathbf{R}})^T (\mathbf{R} - \bar{\mathbf{R}}) \quad j \in \Gamma_{RV} \quad (7)$$

where the mean of these reaction forces is expressed as

$$\bar{R} = \frac{1}{n_r} \sum_j R_j \quad j \in \Gamma_{RV} \quad (8)$$

$n_r$  represents the member numbers of the set  $\Gamma_{RV}$ .  $R_j$  is reaction force at the  $j$ th specific DOF and  $\mathbf{R}$  is the vector consisting of all reaction forces at the specific DOFs.

Obviously,  $D(\mathbf{R})$  is always positive. A small value of  $D(\mathbf{R})$  implies the attainment of a uniform distribution of the reaction forces on the specific DOFs. If  $D(\mathbf{R}) = 0$ , the reaction forces in  $\Gamma_{RV}$  are absolutely the same and distributed uniformly.

### 4 Optimization formulation

Firstly, two formulations are studied comparatively for topology optimization: one is the standard compliance minimization; the other includes the variance of the reaction forces as an additional constraint.

#### 4.1 Formulation 1: minimization of the global compliance

$$\begin{aligned} \text{find} \quad & \mathbf{x} = \{x_i\} \quad i = 1, 2, \dots, n_e \\ \text{min} \quad & C = \mathbf{U}^T \mathbf{K} \mathbf{U} \\ \text{s.t} \quad & \mathbf{F} = \mathbf{K} \mathbf{U} \\ & \sum_i V_i x_i \leq f_U \cdot V \\ & 0 < x_L \leq x_i \leq 1 \end{aligned} \quad (9)$$

Herein,  $\mathbf{x}$  denotes the set of design variables.  $x_i$  represents the presence (1) or absence (0) of the solid material in the  $i^{\text{th}}$  finite element. To avoid the singularity of the structural stiffness matrix in the finite element analysis, a lower bound of  $x_L = 10^{-3}$  is introduced for the design variables. In this formulation,  $n_e$  is the number of designable elements. The upper bound of the volume fraction,  $f_U$ , is defined as the ratio of the upper bound of the volume constraint ( $V_U$ ) to the total volume of all designable elements ( $V$ ) with  $f_U = V_U/V$ .

#### 4.2 Formulation 2: minimization of the global compliance subjected to the variance constraint of the reaction forces

Based on Formulation 1, a variance constraint of reaction forces is introduced and the corresponding optimization problem is stated as

$$\begin{aligned} \text{find} \quad & \mathbf{x} = \{x_i\} \quad i = 1, 2, \dots, n_e \\ \text{min} \quad & C = \mathbf{U}^T \mathbf{K} \mathbf{U} \\ \text{s.t} \quad & \mathbf{F} = \mathbf{K} \mathbf{U} \\ & D(\mathbf{R}) \leq D_U \\ & \sum_i V_i x_i \leq f_U \cdot V \\ & 0 < x_L \leq x_i \leq 1 \end{aligned} \quad (10)$$

Here,  $D_U$ , the upper bound of  $D(\mathbf{R})$ , is usually determined based on the variance of the specific reaction forces obtained in topology optimization using Formulation 1. For example,  $D_U$  can be 20% of  $D(\mathbf{R})$  in topology optimization using Formulation 1.

Additionally, an optimization formulation to minimize the variance of the reaction forces is also studied to identify the extrema of  $D(\mathbf{R})$ .

#### 4.3 Formulation 3: minimization of the variance constraint of the reaction forces

$$\begin{aligned} \text{find} \quad & \mathbf{x} = \{x_i\} \quad i = 1, 2, \dots, n_e \\ \text{min} \quad & D(\mathbf{R}) \\ \text{s.t} \quad & \mathbf{F} = \mathbf{K} \mathbf{U} \\ & \sum_i V_i x_i \leq f_U \cdot V \\ & 0 < x_L \leq x_i \leq 1 \end{aligned} \quad (11)$$

SIMP (Solid Isotropic Material with Penalization) model is used in this work and the penalized Young's modulus is expressed as

$$E_i = x_i^p E^{(0)} \quad (12)$$

in which the superscript (0) indicates the properties of the solid material. The penalty factor  $p=3$  is adopted in this work.

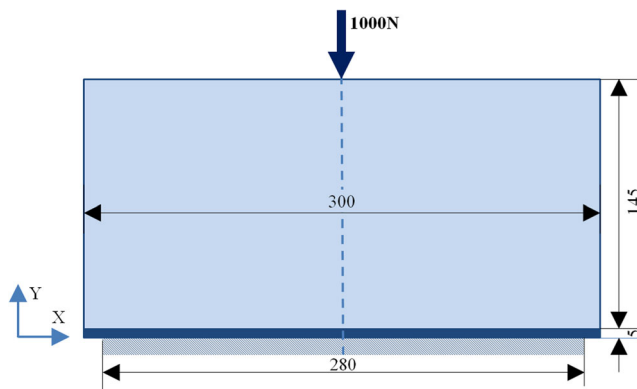


Fig. 2 Structure 1 (unit: mm)

Gradient-based optimizers are usually used to solve topology optimization problems. Therefore, it is necessary to carry out sensitivity analysis with respect to design variables. The sensitivity of the global compliance corresponds to

$$\frac{\partial C}{\partial x_i} = -\mathbf{U}_i^T \frac{\partial \mathbf{K}_i}{\partial x_i} \mathbf{U}_i \tag{13}$$

By means of the adjoint method, the sensitivity of the variance of the reaction forces could be derived by only one additional finite element analysis.

$$\frac{\partial D(\mathbf{R})}{\partial x_i} = \mathbf{\Lambda}^T \frac{\partial \mathbf{K}_{cs}^T}{\partial x_i} \mathbf{U}_c - \lambda^T \frac{\partial \mathbf{K}_{cc}}{\partial x_i} \mathbf{U}_c \tag{14}$$

In (13, 14),  $\frac{\partial \mathbf{K}_i}{\partial x_i}$ ,  $\frac{\partial \mathbf{K}_{cs}^T}{\partial x_i}$  and  $\frac{\partial \mathbf{K}_{cc}}{\partial x_i}$  can be easily derived at the element level. The meanings of the artificial vector  $\mathbf{\Lambda}$  and the adjoint vector  $\lambda$ , and details of the sensitivity analysis are presented in the Appendix.

Fig. 3 Topological configurations in Test 1

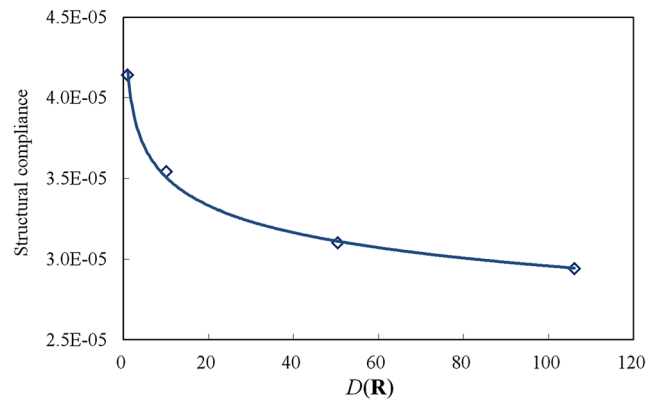
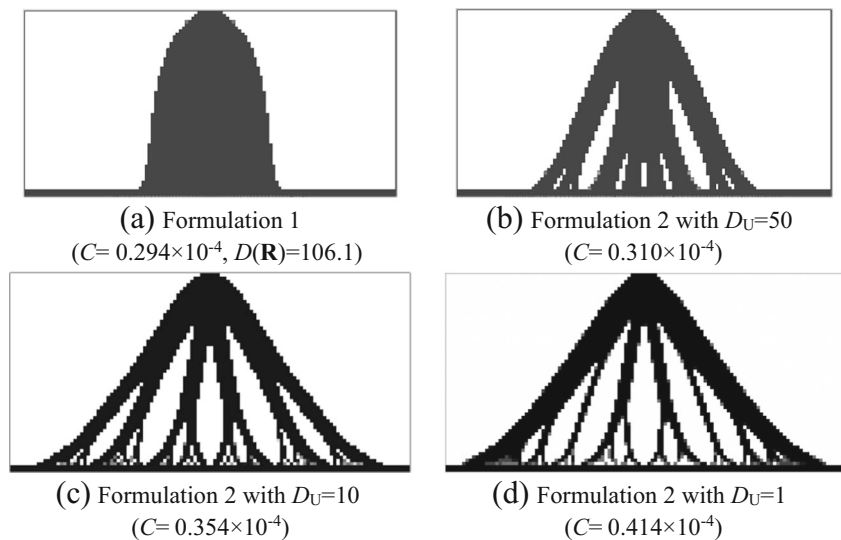
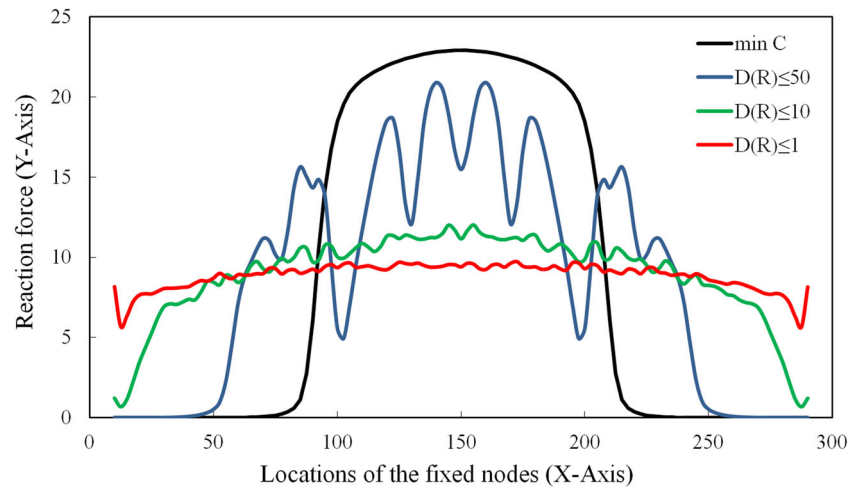


Fig. 4 Relation between the structural compliance and the variance of the specific reaction forces in Test 1

### 5 Numerical tests

In this section, the proposed formulation is tested with several numerical examples. It is assumed that Young’s modulus of the solid material is 105GPa and the Poisson’s ratio is 0.34. Filter methods, including the sensitivity filter (Sigmund 2001) and the density filter (Bourdin 2001), are the most popular regularization methods in the pseudo-density method. A sensitivity filtering technique, whose underlying concepts was rigorously derived from principles in continuum mechanics and nonlocal elasticity (Sigmund and Maute 2012), is adopted herein to yield checkerboard-free topology configuration owing to its ease of application. The ConLin (Convex Linearization) (Fleury and Braibant 1986) is applied to solve the topology optimization problem with the convergence criterion that the relative variations of the objective function and constraints between two consecutive iterations are all less than 0.5%.

**Fig. 5** Distribution of the Y-axis reaction forces in Test 1



**5.1 Test 1**

Consider a plane structure with a non-designable domains (the dark areas), as shown in Fig. 2. The structure is meshed into  $120 \times 60$  four-node finite elements. Each element has a size of 2.5 mm. A vertical force (1000 N) is applied. The upper bound of the volume fraction is  $f_U = 0.3$ . The reaction forces along vertical direction at all fixed nodes are considered.

Fig.3(a) shows the topology optimization result using Formulation 1. The variance of the considered reaction forces is  $D(\mathbf{R}) = 106.1$  for this configuration. In order to realize a more uniform distribution of these reaction forces, Formulation 2 is used with different values of  $D_U$ . Optimized configurations are shown in Fig.3(b)-(d). It is found that the constraint of the variance of reaction forces makes the structure bifurcate, and that smaller values of  $D_U$  produce more refined branches with the reduction of the stiffness of the optimized structures, as shown in Fig.4. It should be noted that in all three tests, the constraints of the material volume and the variance of reaction forces involved in Formulation 2 are both active.

For all tests shown in Fig.3, reaction forces along the vertical direction at all fixed nodes are compared in Fig.5. Obviously, the constraint of the variance of reaction forces makes the applied force be transferred to more fixed nodes and thus reduces the maximum reaction forces greatly.

In the case of  $D_U = 1$ , the reaction forces at all nodes are smoothed into a nearly uniform distribution. The iteration processes of the compliance and  $D(\mathbf{R})$  are plotted in Fig.6. For the considered optimization problem, it is very difficult to find a feasible initial solution. In this paper, the initial values for all design variables are set to be the upper bound of the volume fraction. Clearly, the variance constraint of reaction forces is violated at the beginning. In order to achieve the feasible solutions, the ConLin algorithm combined with the augmented Lagrangian method is utilized. When the iterative solution reaches the upper bound of the variance constraint of reaction forces, it is pushed back into the feasible space and some oscillations occur in the iteration. Finally, both iteration curves converge to the optimized solution.

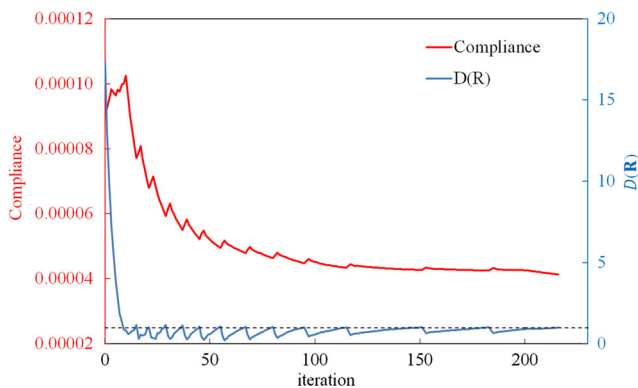


**Fig. 6** Iteration histories of structural compliance and  $D(\mathbf{R})$  (Structure 1,  $D_U = 1$ )

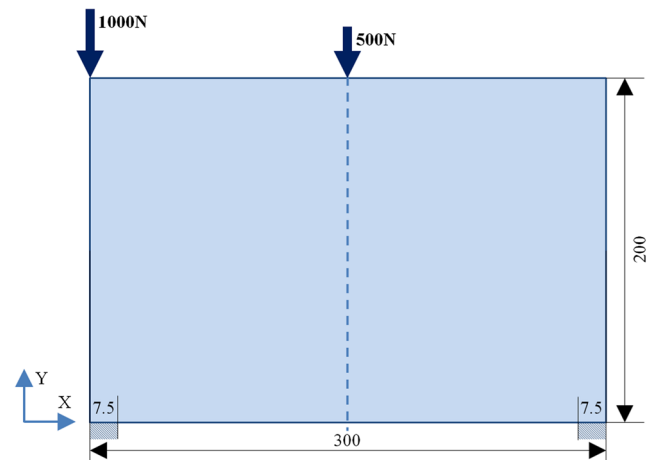
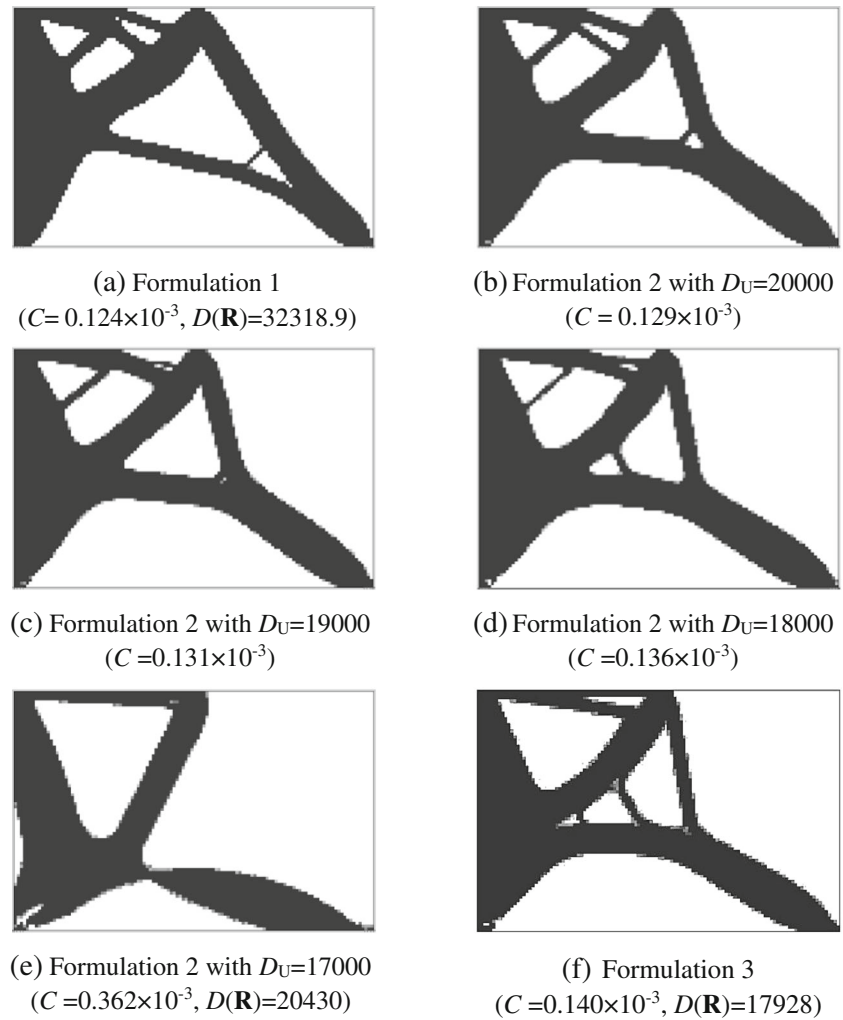


**Fig. 7** Structure 2 (unit: mm)

**Fig. 8** Topological configurations in Test 2

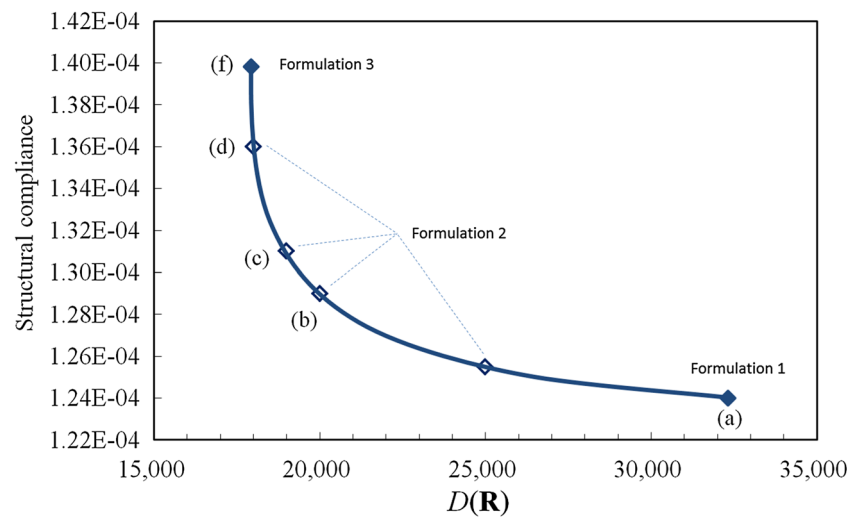


## 5.2 Test 2

A plane structure is clamped on both parts of the bottom and two vertical forces are applied, as shown in Fig. 7. The size of

four-node finite element is 2.5 mm and a mesh of  $120 \times 80$  elements is used. The upper bound of the volume fraction is  $f_U = 0.3$ . The reaction forces along vertical direction at all fixed nodes are considered.

**Fig. 9** Relation between the structural compliance and the variance of the specific reaction forces in Test 2



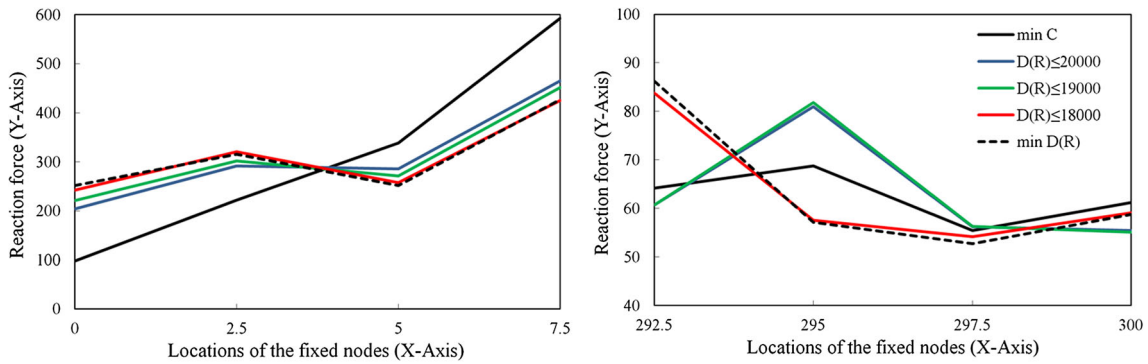


**Fig. 10** Reaction force distributions of Structure 2

Topology optimization results are shown in Fig. 8. Formulation 1 leads to the stiffest configuration and the stiffness of the optimized structures decreases with  $D_U$  if the variance of reaction forces is constrained. Note that the constraints of the material volume and the variance of reaction forces are both active in the tests using Formulation 2.

Here, the case of  $D_U = 17,000$  should be highlighted. The optimized configuration is quite different. Unfortunately,  $D(\mathbf{R})$  cannot decrease below its upper bound  $D_U$  even after 300 iterations in this case. Besides, the structural compliance of this test is clearly larger than others. Further investigation is made here to clarify this case. Using Formulation 3,  $D(\mathbf{R}) = 17,928$  is found as the extrema of the variance of reaction forces, as shown in Fig. 8(f). It means that it is impossible to obtain absolutely uniform distribution of the reaction forces under the prescribed loads and boundary conditions in this test.

Fig. 9 shows the relation between the structural compliance and the variance of specific reaction forces. Around solution (f), the global compliance decreases quickly while the uniformity of the reaction forces increases slightly. Comparatively, around solution (a), the global compliance decreases slowly while the variance of

the reaction forces quickly increases. The reaction forces in vertical direction at all fixed nodes are shown in Fig. 10.

### 5.3 Test 3

The proposed method is now tested for a large-scale engineering problem. The pedestal of a milling machine is shown in Fig. 11. Assume that the dark areas are non-designable. The structure is fixed on the six areas of the bottom and undergoes pressures on several plane surfaces. The whole structure is meshed into 120,558 solid elements. The mass of the whole structures should be less than 1500 kg. The reaction forces along Z-axis at all fixed nodes are considered.

In the design of the pedestal of a milling machine, the stiffness of the whole structure is one of the most important requirements. Therefore, Formulation 1 is firstly utilized to obtain the configuration involving the maximum stiffness and Formulation 2 is then adopted to improve the uniformity of the reaction forces. Fig. 12 illustrates that obvious differences exist between the topology optimization results due to the presence of the variance constraint of the reaction forces. The additional variance constraint reduces the max value and the

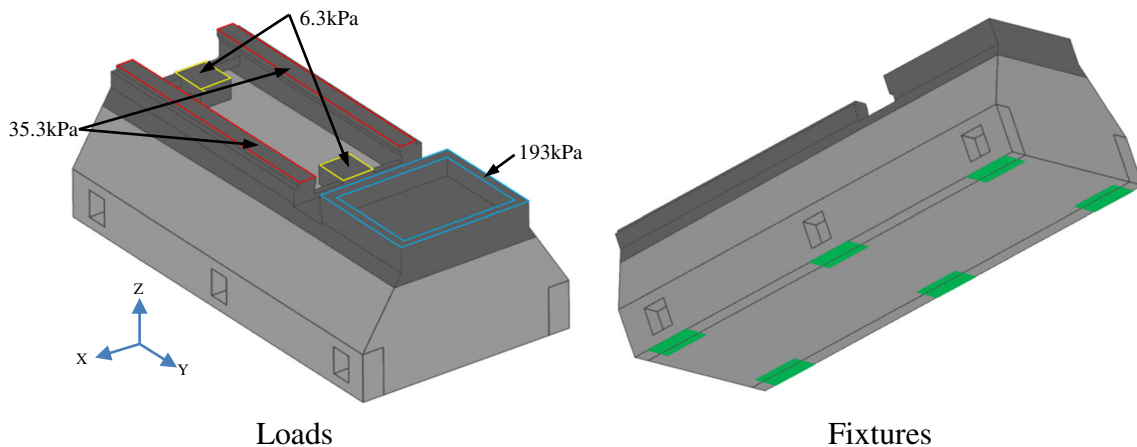
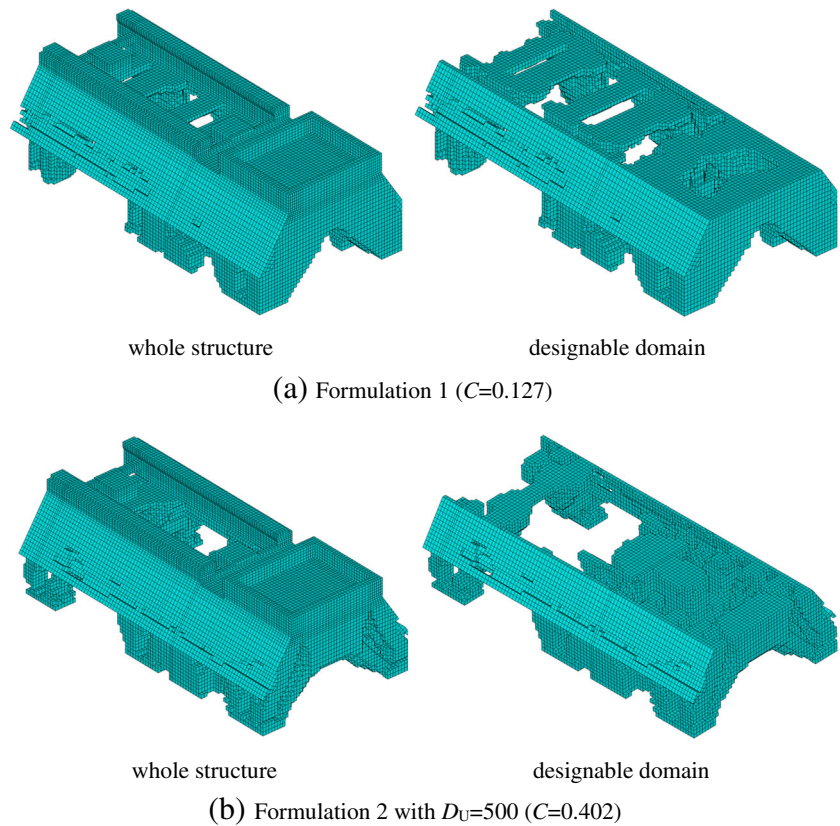


**Fig. 11** Structure 3 (Pedestal of a milling machine)

**Fig. 12** Topological configurations in Test 3



variance of the reaction forces along Z-axis on the supports, as shown in Fig. 13.

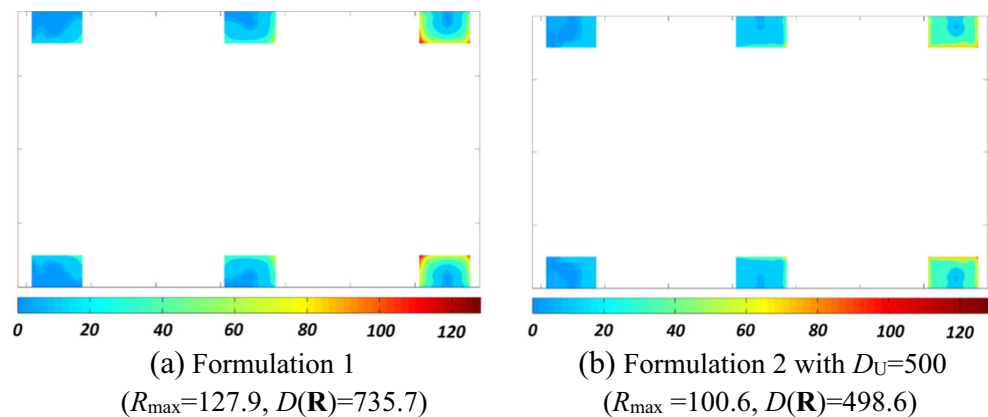
## 6 Conclusions

In topology optimization, the exploration and development of new optimization formulations constructed for various design criteria are of significant engineering importance. In this paper, variance constraint of reaction forces is introduced into structural topology optimization to meet the engineering design needs. The variance of the reaction forces is introduced as the quantitative description of uniformity of these reaction forces

on the fixed nodes. Based on the traditional formulation of the compliance minimization subject to the volume constraint, the variance constraint of the specific reaction forces is added. Its upper bound is determined by a relaxation of the variance value obtained in traditional optimization formulation. Besides, an optimization formulation to minimize the variance of the reaction forces is also studied to identify its extrema. By means of the adjoint method, the sensitivities of the variance of the reaction forces are derived by one additional finite element analysis.

Numerical tests indicate that variance constraint of reaction forces could reduce the maximum value and improve the uniformity of the reaction forces, to some extent. An extrema exists for the variance of reaction forces if the support positions are

**Fig. 13** Reaction force distributions in Test 3





prescribed. Therefore, if the upper bound of the variance constraint of reaction forces is smaller than its extrema, the optimization process might fail to find the optimal solution. In order to further improve the distribution uniformity of the reaction forces, support positions could be included in the optimization formulation as constraints or design variables in future work.

**Acknowledgements** This work is supported by the National Key Research and Development Program of China (2017YFB1102800), the National Natural Science Foundation of China (11672239, 11432011, 11620101002), the Natural Science Basic Research Plan in Shaanxi Province of China (2017JM1002) and the Key Research and Development Program of Shaanxi (S2017-ZDYF-ZDXM-GY-0035)

**Appendix: Sensitivity analysis**

The sensitivity analysis of the global compliance and the variance of reaction forces with respect to design variables is detailed as follow.

**Sensitivity analysis of the global compliance**

Based on the definition of the global compliance, the sensitivity of the latter then corresponds to

$$\frac{\partial C}{\partial x_i} = 2\mathbf{U}^T \frac{\partial \mathbf{F}}{\partial x_i} - \mathbf{U}^T \frac{\partial \mathbf{K}}{\partial x_i} \mathbf{U} = 2\mathbf{U}_c^T \frac{\partial \mathbf{F}^a}{\partial x_i} - \mathbf{U}_i^T \frac{\partial \mathbf{K}_i}{\partial x_i} \mathbf{U}_i \quad (\text{A.1})$$

In this work, the applied forces are supposed to be design-independent. This implies that

$$\frac{\partial \mathbf{F}^a}{\partial x_i} = 0 \quad (\text{A.2})$$

The sensitivity of the global compliance is then rewritten as

$$\frac{\partial C}{\partial x_i} = -\mathbf{U}_i^T \frac{\partial \mathbf{K}_i}{\partial x_i} \mathbf{U}_i \quad (\text{A.3})$$

**Sensitivity analysis of the variance of reaction forces**

Based on the definition in Section 3, the sensitivity of the variance of the specific reaction forces corresponds to

$$\frac{\partial D(\mathbf{R})}{\partial x_i} = \frac{1}{n_r} \sum_j 2(R_j - \bar{R}) \left( \frac{\partial R_j}{\partial x_i} - \frac{\partial \bar{R}}{\partial x_i} \right) \quad (\text{A.4})$$

where the partial derivative of the mean reaction force is expressed as

$$\frac{\partial \bar{R}}{\partial x_i} = \frac{1}{n_r} \sum_{\zeta} \frac{\partial R_{\zeta}}{\partial x_i} \quad (\text{A.5})$$

Thus, we have

$$\begin{aligned} \frac{\partial D(\mathbf{R})}{\partial x_i} &= \frac{1}{n_r} \sum_j 2(R_j - \bar{R}) \left( \frac{\partial R_j}{\partial x_i} - \frac{1}{n_r} \sum_{\zeta} \frac{\partial R_{\zeta}}{\partial x_i} \right) \\ &= \frac{2}{n_r} \sum_j (R_j - \bar{R}) \left( \left(1 - \frac{1}{n_r}\right) \frac{\partial R_j}{\partial x_i} - \frac{1}{n_r} \sum_{\zeta, \zeta \neq j} \frac{\partial R_{\zeta}}{\partial x_i} \right) \end{aligned} \quad (\text{A.6})$$

This expression can be rewritten as

$$\frac{\partial D(\mathbf{R})}{\partial x_i} = \mathbf{\Lambda}^T \frac{\partial \mathbf{R}}{\partial x_i} \quad (\text{A.7})$$

in which  $\mathbf{\Lambda}$  is a vector

$$\mathbf{\Lambda} = \left\{ \begin{array}{c} \Lambda_1 \\ \vdots \\ \Lambda_j \\ \vdots \\ \Lambda_{n_s} \end{array} \right\} \quad (\text{A.8})$$

with each term being calculated by

$$\Lambda_j = \begin{cases} \frac{2}{n_r} \left( (R_j - \bar{R}) \left(1 - \frac{1}{n_r}\right) - \frac{1}{n_r} \sum_{\zeta, \zeta \neq j} (R_{\zeta} - \bar{R}) \right) & j \in \Gamma_{RV} \\ 0 & j \notin \Gamma_{RV} \end{cases} \quad (\text{A.9})$$

To calculate  $\frac{\partial D(\mathbf{R})}{\partial x_i}$ , the partial derivative of the reaction force vector  $\mathbf{R}$  is necessary. According to (6), we have

$$\frac{\partial \mathbf{R}}{\partial x_i} = \frac{\partial \mathbf{K}_{cs}^T}{\partial x_i} \mathbf{U}_c + \mathbf{K}_{cs}^T \frac{\partial \mathbf{U}_c}{\partial x_i} \quad (\text{A.10})$$

and

$$\frac{\partial \mathbf{U}_c}{\partial x_i} = \mathbf{K}_{cc}^{-1} \left( \frac{\partial \mathbf{F}^a}{\partial x_i} - \frac{\partial \mathbf{K}_{cc}}{\partial x_i} \mathbf{U}_c \right) \quad (\text{A.11})$$

Under the assumption of design-independent force (i.e.,  $\frac{\partial \mathbf{F}^a}{\partial x_i} = 0$ ), the above relation can be simplified as

$$\frac{\partial \mathbf{U}_c}{\partial x_i} = -\mathbf{K}_{cc}^{-1} \frac{\partial \mathbf{K}_{cc}}{\partial x_i} \mathbf{U}_c \quad (\text{A.12})$$

The substitution of (A.12) into (A.10) yields

$$\frac{\partial \mathbf{R}}{\partial x_i} = \frac{\partial \mathbf{K}_{cs}^T}{\partial x_i} \mathbf{U}_c - \mathbf{K}_{cs}^T \mathbf{K}_{cc}^{-1} \frac{\partial \mathbf{K}_{cc}}{\partial x_i} \mathbf{U}_c \quad (\text{A.13})$$

Now, the sensitivity of the variance of the considered reaction forces can be derived as

$$\frac{\partial D(\mathbf{R})}{\partial x_i} = \mathbf{\Lambda}^T \frac{\partial \mathbf{K}_{cs}^T}{\partial x_i} \mathbf{U}_c - \mathbf{\Lambda}^T \mathbf{K}_{cs}^T \mathbf{K}_{cc}^{-1} \frac{\partial \mathbf{K}_{cc}}{\partial x_i} \mathbf{U}_c \quad (\text{A.14})$$

in which the adjoint method is applied to calculate the second term.

Suppose

$$\mathbf{\Lambda}^T \mathbf{K}_{cs}^T \mathbf{K}_{cc}^{-1} = \boldsymbol{\lambda}^T \quad (\text{A.15})$$

The adjoint vector  $\boldsymbol{\lambda}$  can then be obtained by

$$\mathbf{K}_{cc} \boldsymbol{\lambda} = \mathbf{K}_{cs} \boldsymbol{\Lambda} \quad (\text{A.16})$$

or

$$\begin{bmatrix} \mathbf{K}_{cc} & \mathbf{K}_{cs} \\ \mathbf{K}_{cs}^T & \mathbf{K}_{ss} \end{bmatrix} \begin{Bmatrix} \boldsymbol{\lambda} \\ \mathbf{0} \end{Bmatrix} = \begin{Bmatrix} \mathbf{K}_{cs} \boldsymbol{\Lambda} \\ \mathbf{R}_\lambda \end{Bmatrix} \quad (\text{A.17})$$

Here,  $\mathbf{R}_\lambda$  is the reaction forces in the additional analysis related to (A.17). Obviously, only one additional finite element analysis needs to be carried out under the same boundary conditions as the original structural analysis in (2) no matter what the adjoint load is.

Thus, by virtue of the adjoint method,  $\frac{\partial D(\mathbf{R})}{\partial x_i}$  is established as

$$\frac{\partial D(\mathbf{R})}{\partial x_i} = \boldsymbol{\Lambda}^T \frac{\partial \mathbf{K}_{cs}^T}{\partial x_i} \mathbf{U}_c - \boldsymbol{\lambda}^T \frac{\partial \mathbf{K}_{cc}}{\partial x_i} \mathbf{U}_c \quad (\text{A.18})$$

In this expression,  $\frac{\partial \mathbf{K}_{cs}^T}{\partial x_i}$  and  $\frac{\partial \mathbf{K}_{cc}}{\partial x_i}$  can be easily derived at the element level.

A particular case should be mentioned herein. If the applied force is constant during optimization and the variance constraint is applied to all fixed nodes, the mean reaction force  $\bar{\mathbf{R}}$  is constant as well. As a result, the derivative of the mean reaction force with respect to all design variables in (A.5) is zero and the sensitivity of the variance of specific reaction forces in (A.4) could be simplified as

$$\frac{\partial D(\mathbf{R})}{\partial x_i} = \frac{1}{n_r} \sum_j 2 \left( R_j - \bar{R} \right) \frac{\partial R_j}{\partial x_i} \quad (\text{A.19})$$

Thus, the artificial vector  $\boldsymbol{\Lambda}$  is simplified as

$$\Lambda_j = \begin{cases} \frac{1}{n_r} \sum_j 2 \left( R_j - \bar{R} \right) & j \in \Gamma_{RV} \\ 0 & j \notin \Gamma_{RV} \end{cases} \quad (\text{A.20})$$

## References

- Bendsøe MP (1989) Optimal shape design as a material distribution problem. *Struct Multidisc Optim* 1:193–202
- Bourdin B (2001) Filters in topology optimization. *Int J Numer Methods Eng* 50:2143–2158
- Buhl T (2002) Simultaneous topology optimization of structure and supports. *Struct Multidisc Optim* 23:336–346

- Chang B, Shi Y, Dong S (1999) Comparative studies on stresses in weld-bonded, spot-welded and adhesive-bonded joints. *J Mater Process Technol* 87:230–236
- Cheng GD, Guo X (1997)  $\epsilon$ -relaxed approach in structural topology optimization. *Struct Optim* 13:258–266
- Díaz AR, Kikuchi N (1992) Solutions to shape and topology eigenvalue optimization problems using a homogenization method. *Int J Numer Methods Eng* 35:1487–1502
- Deaton J, Grandhi R (2013) Stiffening of restrained thermal structures via topology optimization. *Struct Multidisc Optim* 48:731–745
- Deaton J, Grandhi R (2014) A survey of structural and multidisciplinary continuum topology optimization: post 2000. *Struct Multidisc Optim* 49:1–38
- Duysinx P, Bendsøe MP (1998) Topology optimization of continuum structures with local stress constraints. *Int J Numer Methods Eng* 43:1453–1478
- Fleury C, Braibant V (1986) Structural optimization: A new dual method using mixed variables. *Int J Numer Methods Eng* 23:409–428
- Gao T, Zhang WH (2011) A mass constraint formulation for structural topology optimization with multiphase materials. *Int J Numer Methods Eng* 88:774–796
- Hilding D (2000) A heuristic smoothing procedure for avoiding local optima in optimization of structures subject to unilateral constraints. *Struct Multidisc Optim* 20:29–36
- Jog CS (2002) Topology design of structures subjected to periodic loading. *J Sound Vib* 253:687–709
- Kočvara M (1997) Topology optimization with displacement constraints: a bilevel programming approach. *Struct Optim* 14:256–263
- Kono D, Nishio S, Yamaji I, Matsubara A (2015) A method for stiffness tuning of machine tool supports considering contact stiffness. *Int J Mach Tool Manu* 90:50–59
- Liu H, Wu J, Wang Y (2015a) Impact of anchor bolts creep relaxation on geometric accuracy decline of large computer numerical control machine tools. *J Xi'an Jiaotong Univ* 49:14–17
- Liu H, Zhang WH, Gao T (2015b) A comparative study of dynamic analysis methods for structural topology optimization under harmonic force excitations. *Struct Multidisc Optim*:1–13
- Ma ZD, Kikuchi N, Cheng HC (1995) Topological design for vibrating structures. *Comput Methods Appl Mech Eng* 121:259–280
- Neves MM, Rodrigues H, Guedes JM (1995) Generalized topology design of structures with a buckling load criterion. *Struct Multidisc Optim* 10:71–78
- Pedersen P, Pedersen N (2012) Interpolation/penalization applied for strength design of 3D thermoelastic structures. *Struct Multidisc Optim* 1–14
- Rodrigues H, Fernandes P (1995) A material based model for topology optimization of thermoelastic structures. *Int J Numer Methods Eng* 38:1951–1965
- Sigmund O (2001) A 99 line topology optimization code written in Matlab. *Struct Multidisc Optim* 21:120–127
- Sigmund O, Maute K (2012) Sensitivity filtering from a continuum mechanics perspective. *Struct Multidisc Optim* 46:471–475
- Sigmund O, Maute K (2013) Topology optimization approaches: A comparative review. *Struct Multidisc Optim* 48:1031–1055
- Takezawa A, Nishiwaki S, Izui K (2006) Structural optimization based on topology optimization techniques using frame elements considering cross-sectional properties. *Struct Multidisc Optim* 34:41–60
- Zhang J, Wang B, Niu F, Cheng G (2015a) Design optimization of connection section for concentrated force diffusion. *Mech Based Des Struct Mach* 43:209–231

- Zhang WH, Yang JG, Xu YJ, Gao T (2014) Topology optimization of thermoelastic structures: mean compliance minimization or elastic strain energy minimization. *Struct Multidisc Optim* 49:417–429
- Zhang WH, Liu H, Gao T (2015b) Topology optimization of large-scale structures subjected to stationary random excitation: An efficient optimization procedure integrating pseudo excitation method and mode acceleration method. *Comput Struct* 158:61–70
- Zhu JH, Zhang WH, Beckers P (2009) Integrated layout design of multi-component system. *Int J Numer Methods Eng* 78:631–651
- Zhu JH, Zhang WH, Xia L (2015) Topology optimization in aircraft and aerospace structures design. *Arch Comput Method E*:1–28
- Zhu JH, Li Y, Zhang WH, Hou J (2016) Shape preserving design with structural topology optimization. *Struct Multidisc Optim* 53:893–906